Electronic Supplementary Material (ESI)
for

In Vitro and In-silico Anticancer Activities of Mn(II), Co(II), and Ni(II) Complexes: Synthesis, Characterizations, Crystal structures, and DFT Studies

M. K. Gond[a], Shivendra kumar Pandey[a], R. Singh[b], Manoj K. Bharty[a]*, Partha Pratim Manna[b]*, V. K. Singh[c], B. Maiti[a], L. B. Prasad[a], R. J. Butcher[d]

[a] *Department of Chemistry, Banaras Hindu University, Varanasi-221005, India*

[b] *Department of Zoology Banaras Hindu University, Varanasi-221005, India*

[c] *School of Biotechnology, Banaras Hindu University, Varanasi-221005, India*

[d] *Department of Chemistry, Howard University, 525 College Street NW, Washington, DC 20059, USA*

*Corresponding author E-Mail: manoj_vns2005@yahoo.co.in; mkbharty@bhu.ac.in

Contents

1. Materials and Methods:

1.1 Chemical and starting materials

Commercial reagents were used without further purification and all experiments were carried out in open atmosphere. Phenyl isothiocyanate and furoic acid hydrazide (Sigma Aldrich), were used as received. All the synthetic manipulations were carried out in open atmosphere and at room temperature. The solvents were dried and distilled before use following the standard procedure. Cis-platin of pharmaceutical grade was purchased from KLAB, Mumbai, India and used as external reference.

1.2 Physical measurements

Carbon, hydrogen and nitrogen contents were estimated on a CHN Model CE-440 Analyser. The electronic spectra were recorded on a SHIMADZU 1700 UV-Vis spectrophotometer. The fluorescent data were collected at room temperature on "Agilent Technologies Cary Eclipse" Fluorescence Spectrophotometer in DMSO. IR spectra were recorded in the 4000-400 cm^{-1} region as KBr pellets on a Varian Excalibur 3100 FT-IR spectrophotometer. Magnetic susceptibility measurements were performed at room temperature on a Cahn Faraday balance using $Hg[Co(NCS)_4]$ as the calibrant. ^{1}H and ^{13}C NMR spectra were recorded in DMSO-d_6 on a JEOL JNM- ECZ500R/S1 FT-NMR spectrometer using TMS as an internal reference. HRMS studies were performed using SCIEX Model-X500R QTOF.

2. X-ray crystallography

Crystals suitable for X-ray analyses of complexes **1**, **2,** and **3** were grown at room temperature. X-ray diffraction data were measured obtained at 293(2) K on an Oxford Diffraction Gemini diffractometer equipped with CrysAlis Pro., using a graphite mono-chromated Mo Kα (λ = 0.71073 Å) radiation source. A semi-empirical multi scan absorption correction was applied to the X-ray data of both compounds. The structure was solved by direct methods (SHELXL-13) and refined by full matrix least-square on F^2 (SHELXL) using anisotropic displacement parameters for all non-hydrogen atoms. All hydrogen atoms were included in calculated position and refined with a riding model [1]. Figures were drawn using the programs MERCURY and ORTEP-3 [2, 3].

Supporting Table ST1. Interatomic distances (Å) and angles (°) [Mn(pfth)$_2$(*o*-phen)] (**1**)

Bond length (Å)			**Bond angles (°)**		
	(Exp.)	**(Cal.)**		**(Exp.)**	**(Cal.)**
Mn(1)-O(1A)	2.190(8)	2.181	O(1A)- Mn1 –O(1A)	157.17(5)	157.67
Mn(1)-N(2A)	2.255(10)	2.299	O(1A)- Mn1- N(2A)	74.06(3)	73.71
Mn(1)-N(4A)	2.267(11)	2.309	O(1A)- Mn1 –N(2A)	92.49(3)	90.03
S(1)-C(7A)	1.703(13)	1.729	N(2A)- Mn1- N(2A)	108.49(6)	107.92
O(1A)-C(8A)	1.271(15)	1.276	O(1A)- Mn1 –N(4A)	106.94(4)	103.23
N(1A)-C(7A)	1.364(15)	1.372	O(1A) -Mn1- N(4A)	91.51(3)	94.79
N(1A)-C(1A)	1.413(15)	1.413	N(2A)- Mn1- N(4A)	91.68(4)	91.39
N(2A)-N(3A)	1.388(14)	1.378	N(2A)- Mn1- N(4A)	155.36(4)	157.72
N(3A)-C(8A)	1.313(15)	1.329	N(4A)- Mn1- N(4A)	73.20(5)	72.39
N(2A)-C(7A)	1.343(15)	1.345	C(8A)- O(1A)- Mn1	114.76(7)	115.72
O(2A)-C(9A)	1.373(16)	1.371	C(7A)- N(2A)- N(3A)	112.05(10)	114.09
N(4A)- C(17A)	1.361(16)	1.358	N(3A)- N(2A)- Mn1	109.42(7)	108.83
N(4A)-C(13A)	1.325(15)	1.329	C(8A)- N(3A)- N(2A)	119.58(10)	119.96
O(2A)-C(12A)	1.370(16)	1.361	N(2A)- C(7A)- S(1)	124.07(9)	123.96

Supporting Table ST2. Intermolecular interactions [Å and º] for [Mn(pfth)$_2$(*o*-phen)] (**1**)

D-H···A	d(D-H)	d(H···A)	d(D···A)	<(DHA)
N(1A)-H(1A)···O(1A)	0.857	2.10	2.9539(14)	172.3
N(3A)-H(3A)··· S(1)	0.93	2.23	2.8221(11)	120.7
C(2A)- H(2AA)···S(2)	0.95	3.00	3.7683(15)	138.9
C(10A)-H(10A)···O(1WB)	0.95	2.30	3.140(8)	146.6
C(12A)- H(12A)···O(1C)	0.95	2.59	3.5219(18)	165.4
C(13A)-H(13A)···S(2)	0.95	2.85	3.4646(13)	123.3
C(14A)-H(14A)···S(2)	0.95	2.78	3.4157(13)	125.3
N(1B)- H(1B)···O(1B)	0.82	2.12	2.9456(15)	173.2
N(3B)-H(3B)···S(2)	0.89	2.41	2.8666(11)	111.6
C(2B) –H(2BA)···S(2)	0.95	2.75	3.2754(15)	115.3
C(2B)- H(2BA)···O(1WD)	0.95	2.54	3.373(10)	146.4
N(1C) –H(1C)···O(1C)	0.84	2.19	3.0285(14)	168.0
N(3C)- H(3C)···S(3)	0.87	2.38	2.8788(12)	116.0
O(1WB)-H(1W3)···O(1WB)	0.82	2.64	3.104(15)	117

Symmetry transformations used to generate equivalent atoms: #1 -x+1,y,-z+1/2 #2 -x+1,-y+1,-z+1 #3 x,y+1,z

Supporting Table ST3. Interatomic distances (Å) and angles (°) for [Co(pfth)$_2$(en)] (**2**)

Bond length (Å)			Bond angles (°)		
	(Exp.)	**(Cal.)**		**(Exp.)**	**(Cal.)**
Co-O(1)	2.072(2)	2.146	O(1)-Co-N(4)	91.31(12)	101.23
Co-N(4)	2.081(3)	2.199	O(1)#1-Co-N(4)	91.65(11)	87.21
Co-N(2)	2.101(3)	2.167	N(4)-Co-N(4)#1	82.90(18)	78.66
S(1)-C(7)	1.698(4)	1.728	O(1)-Co-N(2)	79.50(10)	76.90
O(1)-C(8)	1.271(4)	1.275	O(1)#1-Co-N(2)	97.78(10)	96.41
N(1)-C(7)	1.374(4)	1.369	N(4)-Co-N(2)	92.01(12)	90.56
N(1)-C(1)	1.408(4)	1.413	N(4)#1-Co-N(2)	169.72(12)	158.76
N(2)-C(7)	1.335(4)	1.347	N(2)-Co-N(2)#1	94.35(17)	104.98
N(2)-N(3)	1.385(4)	1.379	C(8)-O(1)-Co	111.7(2)	112.80
N(3)-C(8)	1.321(4)	1.331	C(7)-N(2)-N(3)	113.1(3)	114.42
N(4)-C(13)	1.480(5)	1.480	C(7)-N(2)-Co	139.0(2)	135.65

Supporting Table ST4. Intermolecular interactions [Å and º] for [Co(pfth)$_2$(en)] (**2**)

D-H···A	d(D-H)	d(H···A)	d(D···A)	<(DHA)
N(1)-H(1A)···O(1)#1	0.88	2.10	2.941(4)	158.6
N(3)-H(3B)···S(1)	0.88	2.39	2.842(3)	112.3
N(4)-H(4C)···S(1)#2	0.91	2.55	3.441(3)	167.3
C(6)-H(6A)···S(1)	0.95	2.70	3.254(4)	117.6
C(13)-H(13B)···S(1)#3	0.99	2.91	3.855(4)	159.4

Symmetry transformations used to generate equivalent atoms: #1 -x+1, y, -z+1/2 #2 -x+1, -y+1, -z+1 #3 x, y+1, z

Supporting Table ST5. Interatomic distances (Å) and angles (°) for [Ni(pfth)$_2$(en)] (**3**)

Bond length (Å)			Bond angles (°)		
	(Exp.)	**(Cal.)**		**(Exp.)**	**(Cal.)**
S(1)-C(7)	1.699(4)	1.731	O(1)-Ni-O(1)#1	176.09(14)	174.32
N(1)-C(7)	1.373(4)	1.373	O(1)-Ni-N(4)	91.29(11)	92.92
C(8)-N(3)	1.324(4)	1.329	O(1)-Ni-N(2)	79.53(10)	78.22
N(2)-C(7)	1.333(4)	1.341	N(4)-Ni-N(2)	92.06(12)	90.82
O(1)-C(8)	1.268(4)	1.278	O(1)-Ni-N(2)#1	97.78(10)	98.02
N(2)-N(3)	1.385(4)	1.378	N(4)#1-Ni-N(2)#1	92.06(12)	90.82
Ni-O(1)	2.072(2)	2.100	C(8)-O(1)-Ni	111.8(2)	112.33
Ni-N(4)	2.082(3)	2.139	C(7)-N(2)-Ni	139.1(2)	136.91
Ni-N(2)	2.101(3)	2.157	N(3)-N(2)-Ni	107.8(2)	107.60
N(1)-C(1)	1.409(4)	1.409	N(4)#1-Ni-N(4)	82.83(17)	81.57
N(3)-C(8)	1.324(4)	1.329	N(4)#1-Ni-N(2)	169.73(12)	166.84

Symmetry transformations used to generate equivalent atoms: #1 -x+1, y, -z+1/2

Supporting Table ST6. Intermolecular interactions [Å and º] for [Ni(pfth)$_2$(en)] (**3**)

D-H···A	d(D-H)	d(H···A)	d(D···A)	<(DHA)
N(1)-H(1A)...O(1)#1	0.88	2.10	2.941(4)	158.6
N(3)-H(3B)...S(1)	0.88	2.39	2.842(3)	112.3
N(4)-H(4C)...S(1)#2	0.91	2.55	3.441(3)	167.3
C(6)-H(6A)...S(1)	0.95	2.70	3.254(4)	117.6
C(13)-H(13B)...S(1)#3	0.99	2.91	3.855(4)	159.4

Symmetry transformations used to generate equivalent atoms: #1 -x+1, y, -z+1/2 #2 -x+1, -y+1, -z+1 #3 x, y+1, z

3. H-Bonding interaction Figures

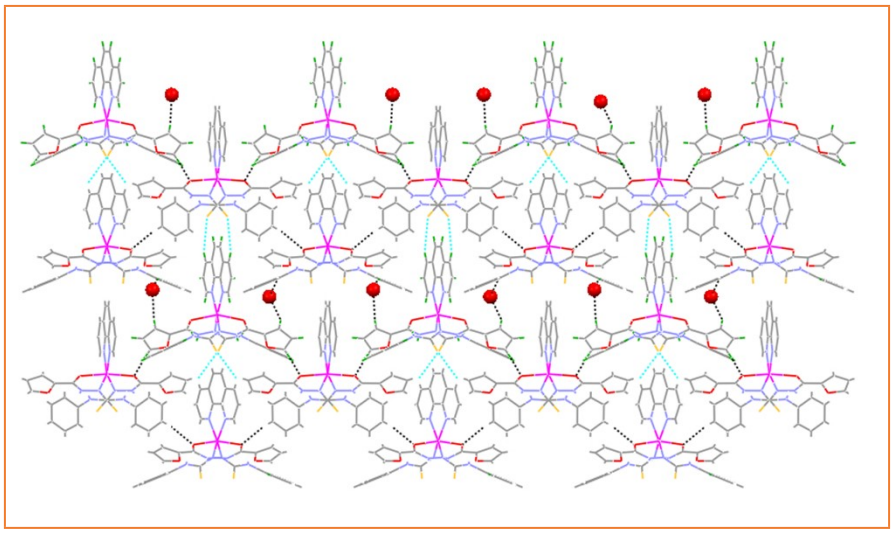

Fig. S1. Showing intermolecular C-H···S and C-H···O hydrogen bonding leading to a butterfly like architecture in complex **1**

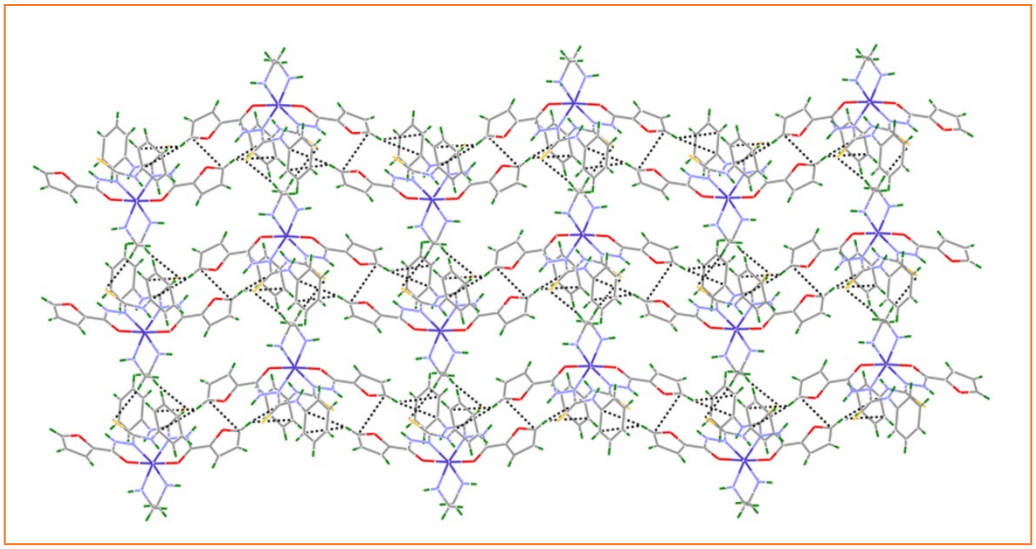

Fig. S2. Showing intermolecular N-H··S hydrogen bonding leading to supramolecular architecture in complex **2**

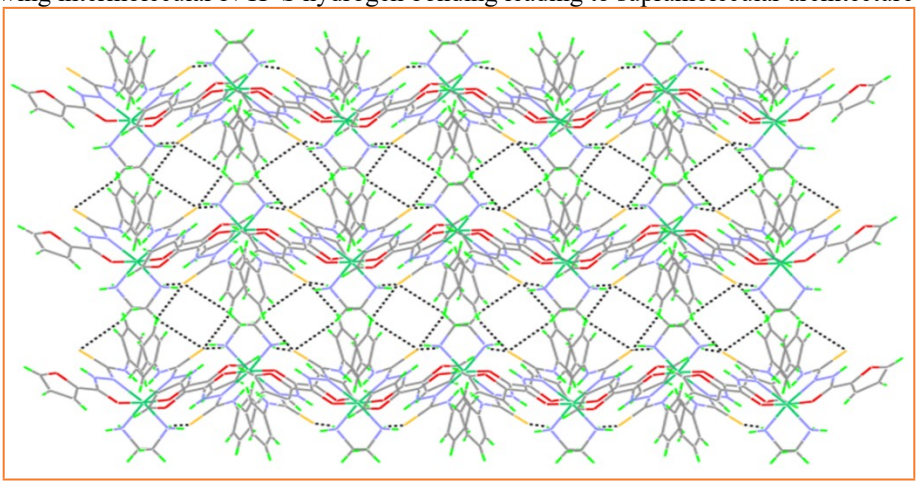

Fig. S3. Showing intermolecular N-H··S hydrogen bonding leading to a butterfly like structure in complex **3**

4. π-π stacking interaction

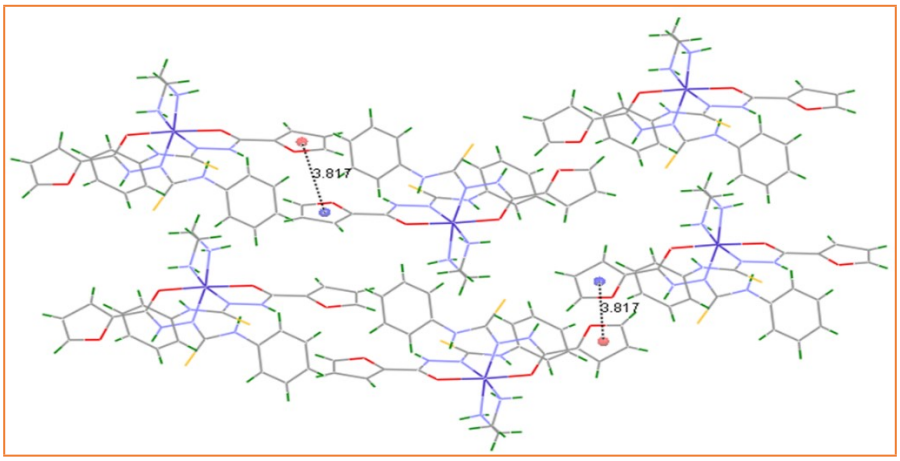

Fig. S4. Showing intermolecular π···π stacking interaction between two furan rings of complex **2**

5. Quantum Chemical Calculations

To understand the binding sites and to verify the composition of the complexes, Density Functional Theory (DFT) calculations have been performed. In these calculations, B3LYP density functional theory method has been used which is a hybrid version of DFT and Hartree-Fock (HF) methods [4]. In this method, the exchange energy from Becke's exchange functional is combined with the exact energy from Hartree-Fock theory [5]. The three parameters define the hybrid functional, specifying how much of the exact exchange is mixed in along with the component exchange and correlation functionals [6]. The 6-31G** basis set for all the atoms except metal ions have been used. The LanL2DZ basis set with an effective core pseudo potential has been used for the metal atom [7]. All the geometry optimizations and frequency calculations (to verify a genuine minimum energy structure) were performed using Gaussian 09 program package [8]. The electronic excitation energies and intensities of the three lowest-energy spin allowed transitions were calculated using the time dependent density functional theory (TD-DFT). It is worth pointing out here that the starting geometries were chosen based on X-ray crystallographic structures with required modification for the computations if needed.

6. Molecular docking Analysis

Three target proteins 6NE5: Myeloid Cell Leukemia-1 (Mcl-1), 6E91: Carbonic anhydrase IX (CA IX), and 6H0W: Lysine Demethylase 4D were selected as a potential target for docking calculation.

6.1 Receptors collection and structures refinement

The target proteins structures (MCL-1, KDM4D and CAIX) were chosen for the docking calculations. The target structures PDB IDs (6NE5, 6H0W and 6E91) were downloaded from the Protein Data Bank (PDB; http://www.rcsb.org/pdb/home/home.do) [9]. The refined and verified crystal structures of the target proteins were taken for the docking studies (PDB ID: 6NE5, 6H0W and 6E91) (*Fig. S5*). The target structures were optimized for further process.

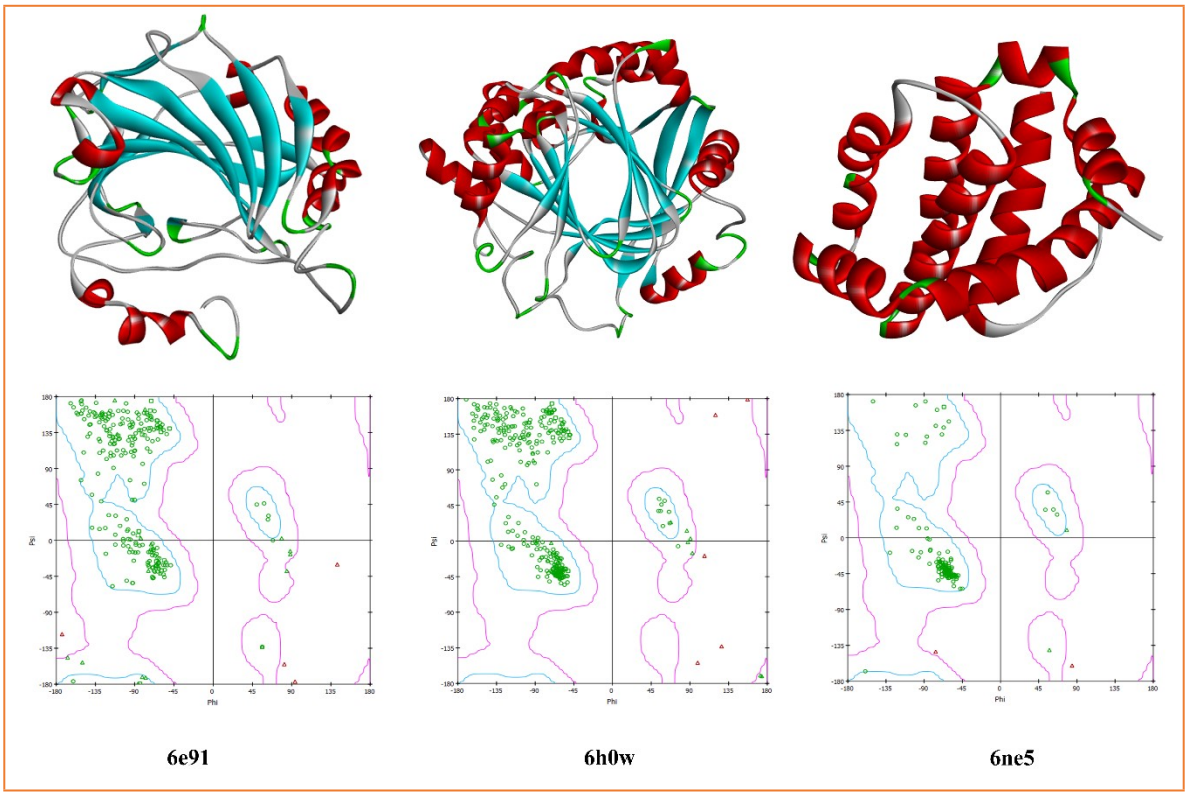

Fig. S5 Target receptors with their Ramachandran plot

6.2 Ligand selection and optimization

The ligand 4-phenyl-(2-furoyl)-thiosemicarbazide (Hpfth) and other ligands associated with its metal complexes were selected for screening, based on comprehensive literature survey for newly synthesized compounds with anti-tumour activity. Ligand structures were drawn using the GAUSSVIEW software whereas Cif files were used for geometric optimization of

metal complexes (Fig. S7). Further optimized structures were used for molecular docking calculation. Minimization by geometric optimization using GAUSSVIEW is carried out for selected ligands to correct bond orders and bond angles.

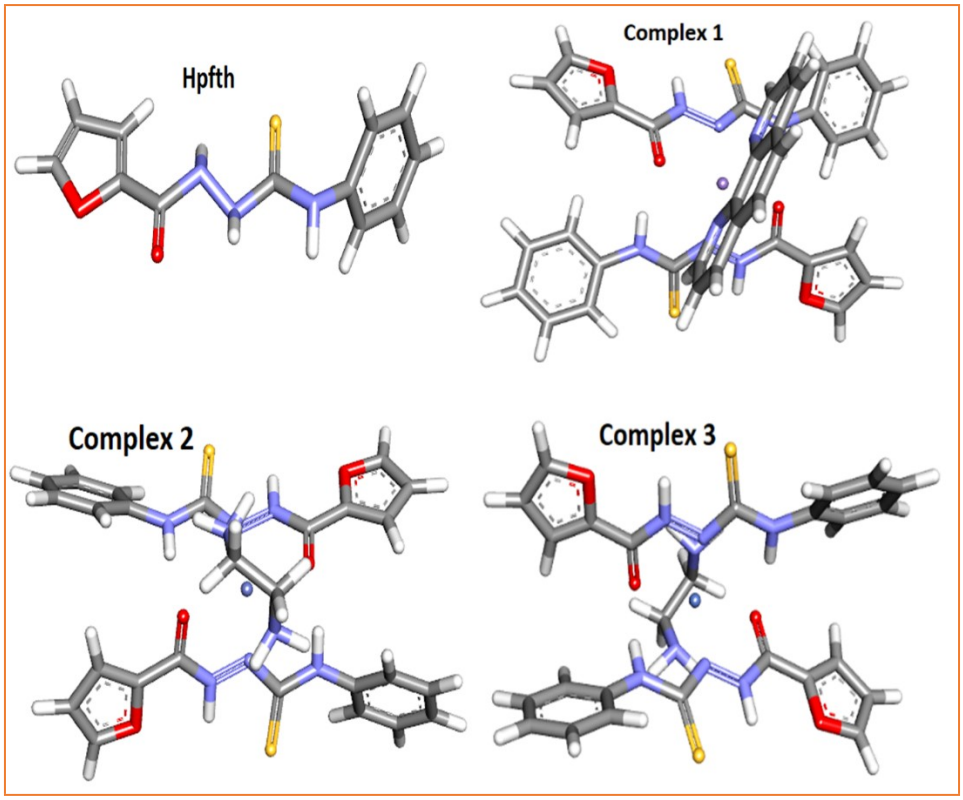

Fig. S6. DFT optimised structures of Hpfth and complexes **1**, **2**, and **3**

6.3 Active site identification

The refine structures of PDB ID: 6NE5, 6H0W and 6E91 were further used for active sites and their residues identification. The active sites were predicted for selected structures using metaPocket 2.0 server. The metaPocket server is a meta server to identify ligand binding sites on protein surface based on a consensus method, in which the predicted binding sites from eight methods: QSiteFinder, LIGSITEcs, PASS, Fpocket, SURFNET, GHECOM, ConCavity and POCASA are combined together to improve the prediction success rate [10]. (*Table ST7*)

Table ST7. Active site analysis of protein

S.N.	Protein PDB ID	Binding site 1	Binding site 2	Binding site 3
1.	6NE5	Met250, Val253, Phe254, Arg263, Leu267, Met231, Val249, Leu246, Thr266, Leu235, Ser247, Arg248, Ser245, Phe270, Ile294, Leu290, Gly271, Phe228, Ala227, Val274, His224, Ile237, Ser293	Lys194, Asp195, Thr196, Pro198, Met199, Gly203, Ala204, Arg207, Gly200, Arg184, Lys197, Leu210, Arg214, Glu211, Lys208, Glu188	Val307, Arg310, Gly311, Leu306, Gln177, Trp312, Asp313, Leu174, Glu173, Ser202, Glu317, Thr205
2.	6E91	Gln103, Asp243, Trp245, Tyr7, Val242, Pro247, Pro13, Phe231, Leu240, Asn244, Trp5, Asn62, Gly63, His64, Glu170, His4, Gly8, Gly6, Glu239, Gly12, Asn232, Gly233, Glu14, Glu236, Lys9, Asn11, Glu238, His10	Val143, Leu198, Thr199, Val207, Trp209, Val121, Leu141, His94, His119, Thr200, His96, Tyr7, His64, Ser65, Asn62, Gln67, Gln92, Asn244, Leu91, Val131, Val135, Pro201, Phe93, Trp5, Pro202	Ala54, Asn178, Phe179, Asp180, Pro181
3.	6H0W	Gln309, Cys310, Ser311, Ala315, Trp336, Gln340, Arg243, Met321, Arg316, Val317, His244, Glu314, Val246, Ala240, Gly313, Asp195, Tyr89, Gln88, Met196, His90, Lys245, Leu242, Lys92, His192, Thr193, Glu194, Thr318, Trp191, Phe324, Leu198, Ser320, Leu75, Lys91, Asn294, Thr73, Asp139, Tyr179, Val175, Ile160, Ala190, Phe319, Gln161, Asn176, Gln77, Thr188, Phe189, Ala138, Thr177, Tyr181, His280, Tyr136, Ser141, Ile293, Ser200, Ala292, Thr274, Trp212, Asn202, Lys210, Asn284, Ala290, Gln266, Leu204, Ala72, Ile71, Ile140, Leu70	Gln221, Glu224, Tyr277, Ser308, Met306, His192, Thr193, Leu242, Arg243, Tyr279, Trp191, Lys245, Ala240, Phe241, Gly239, Arg228, Ser235, Cys238, Ala227, Asp195, Asp197, Ala307, Tyr303, Pro217, Glu218, Gln309, Cys310, Arg332, Lys305, Asp302, Pro276	Tyr63, Tyr203, His205

6.4 Docking calculation

For molecular docking calculation of ligand 4-phenyl-(2-furoyl)-thiosemicarbazide (Hpfth) and its associated metal complexes [Mn(pfth)$_2$(*o*-phen)] (**1**), [Co(pfth)$_2$(en)] (**2**) and [Ni(pfth)$_2$(en)] (**3**) were used (Table ST8). Candidate targets PDB ID: 6NE5, 6H0W and 6E91 were used for docking analysis using PachDock online server (https://bioinfo3d.cs.tau.ac.il/ PatchDock/) [11]. The PachDock algorithm ranked the docked complexes on the basis of geometrical shape complementary scores (Fig. S7 and S8). The interacted amino acid residues with ligand atoms who were involved in hydrogen bonding were analysed and visualized using BIOVIA Discovery Studio 2019 suite (https://discover.3ds.com/discovery-studio-visualizer-download) (Fig. S9 and S10).

Table ST8. Docking calculation data of ligand and complexes

S.N.	Ligand/ Complex	Protein Name/PDB ID	Score	Area	ACE	Transformation	Interacted residues	Site Interaction
1.	**Hpfth**	**MCL-1/ 6ne5**	4208	465.30	-288.95	-1.90 0.00 -1.28 -2.99 -21.19 89.19	Met231, Leu235, Leu246, Val249, Met250, Val253, Phe254, Arg263, Thr266, Leu267	Binding Site 1: Met231, Leu235, Leu246, Val249, Met250, Val253, Phe254, Arg263, Thr266, Leu267
2.	**1**		5710	887.00	-692.88	2.30 0.74 -2.79 -6.24 -18.63 92.99	Ala227, Phe228, Met231, Leu246, Val249, Met250, His252, Val253, Phe254, Arg263, Leu267, Phe270, Gly271	Binding Site 1: Ala227, Phe228, Met231, Leu246, Val249, Met250, Val253, Phe254, Arg263, Leu267, Phe270, Gly271
3.	**2**		5474	848.50	-663.61	0.69 1.06 2.04 -5.08 -17.91 91.63	Ala227, Phe228, Met231, Leu235, Leu246, Val249, Met250, Val253, Phe254, Arg263, Leu267, Phe270, Leu290	Binding Site 1: Ala227, Phe228, Met231, Leu235, Leu246, Val249, Met250, Val253, Phe254, Arg263, Leu267, Phe270, Leu290
4.	**3**		5538	748.70	-429.41	1.14 -1.34 -1.59 -4.67 -16.69 95.49	His224, Ala227, Met231, Leu235, Val249, Met250, His252, Val253, Phe254, Gly262, Arg263, Thr266, Leu267, Phe270, Gly271	Binding Site 1: His224, Ala227, Met231, Leu235, Val249, Met250, Val253, Phe254, Arg263, Thr266, Leu267, Phe270, Gly271
5.	**Hpfth**	**KDM4D/ 6h0w**	4358	543.60	-93.15	-0.01 -0.97 2.97 -10.17 -14.16 -20.79	Gln88, His90, Tyr136, Asp139, Tyr181, Phe189, Asn202, Lys210, Trp212, Lys245	Binding Site 1: Gln88, His90, Tyr136, Asp139, Tyr181, Phe189, Asn202, Lys210, Trp212, Lys245
6.	**1**		7042	926.50	-175.42	-2.80 0.10 0.69 -9.04 -11.49 -13.32	Leu75, His90, Tyr136, Asp139, Val146, Tyr179, Tyr181, Glu194, Asp195, Ser200, Asn202, His244, Lys245, Asn294, Glu314, Ala315, Arg316, Val317	Binding Site 1: Leu75, His90, Tyr136, Asp139, Tyr179, Tyr181, Glu194, Asp195, Ser200, Asn202, His244, Lys245, Asn294 Glu314, Ala315, Arg316, Val317 Binding Site 2: Asp195, Lys245
7.	**2**		7304	868.10	-88.03	2.77 0.98 -3.06 -7.51 -8.30 -12.79	Tyr136, Asp139, Asn176, Phe189, His192, Thr193, Glu194, Asp195, Asn202, Trp212, Lys245, His280, Ala292, Asn294, Val317, Thr318, Ser320	Binding Site 1: Tyr136, Asp139, Asn176, Phe189, His192, Thr193, Glu194, Asp195, Asn202, Trp212, Lys245, His280, Ala292, Asn294, Val317, Thr318, Ser320 Binding Site 2: His192, Thr193 Asp195, Lys245
8.	**3**		7294	913.80	-131.85	3.13 -1.15 -0.43 -6.97 -8.16 -12.32	Tyr136, Asp139, Asn176, Tyr179, Tyr181, Phe189, His192, Glu194, Asp195, Asn202, Lys245, His280, Ala292, Ile293, Asn294, Thr318, Ser320	Binding Site 1: Tyr136, Asp139, Asn176, Tyr179, Tyr181, Phe189, His192, Glu194, Asp195, Asn202, Lys245, His280, Ala292, Ile293, Asn294, Thr318, Ser320 Binding Site 2: His192, Asp195, Lys245
9.	**Hpfth**	**CAIX/ 6e91**	3874	428.60	-233.42	-1.45 0.91 0.86 -2.32 11.52 18.39	Leu91, His94, Val121, Val131, Gly132, Val135, Val143, Leu198, Thr199, Thr200, Trp209	Binding Site 2: Leu91, His94, Val121, Val131, Val135, Val143, Leu198, Thr199, Thr200, Trp209
10.	**1**		6172	774.30	-292.85	0.35 -0.18 -1.78 9.09 -3.79 6.02	His4, Trp5, Gly8, His10, Asn11, Asn62, His64, Phe231, Asn232, Glu236, Glu239	Binding Site 1: His4, Trp5, Gly8, His10, Asn11, Asn62, His64, Phe231, Asn232, Glu236, Glu239, Binding Site 2: Trp5, Asn62, His64
11.	**2**		5666	689.50	-225.71	2.97 0.13 -1.22 6.87 -2.96 5.06	His4, Tyr7, His10, Asn11, Gly63, His64, Glu170, Phe231, Asn232, Gly233, Glu236, Glu239	Binding Site 1: His4, Tyr7, His10, Asn11, Gly63, His64, Glu170, Phe231, Asn232, Gly233, Glu236, Glu239, Binding Site 2: Tyr7, His64
12.	**3**		6018	686.90	-217.39	-2.93 -0.20 1.94 7.62 -4.47 5.17	His4, Trp5, Gly6, His10, Asn11, Gly63, His64, Glu170, Phe231, Asn232, Glu236, Glu239	Binding Site 1: His4, Trp5, Gly6, His10, Asn11, Gly63, His64, Glu170, Phe231, Asn232, Glu236, Glu239 Binding Site 2: Trp5, His64

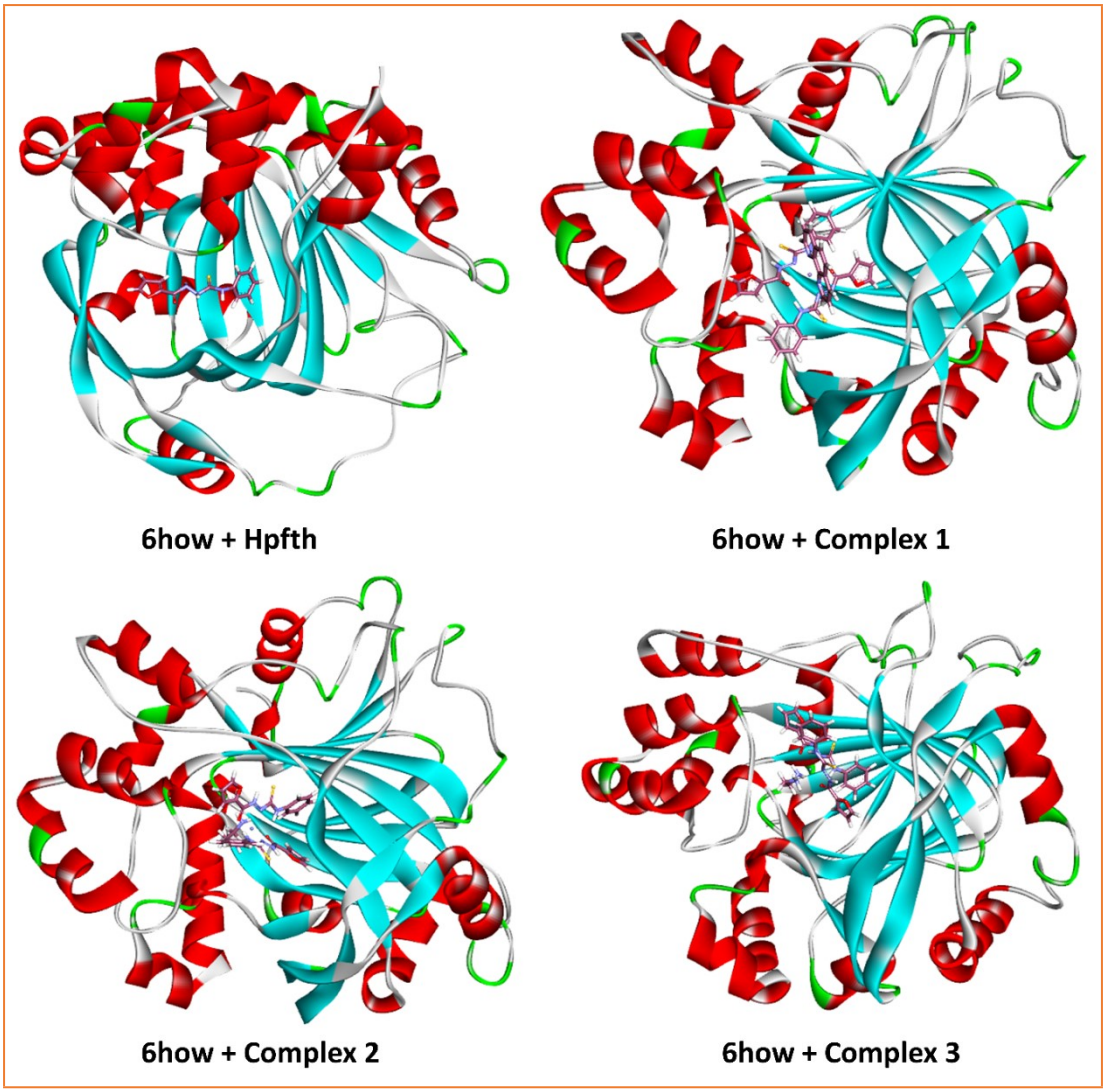

Fig. S7. Docking of Hpfth and complexes with candidate selected target protein 6h0w.

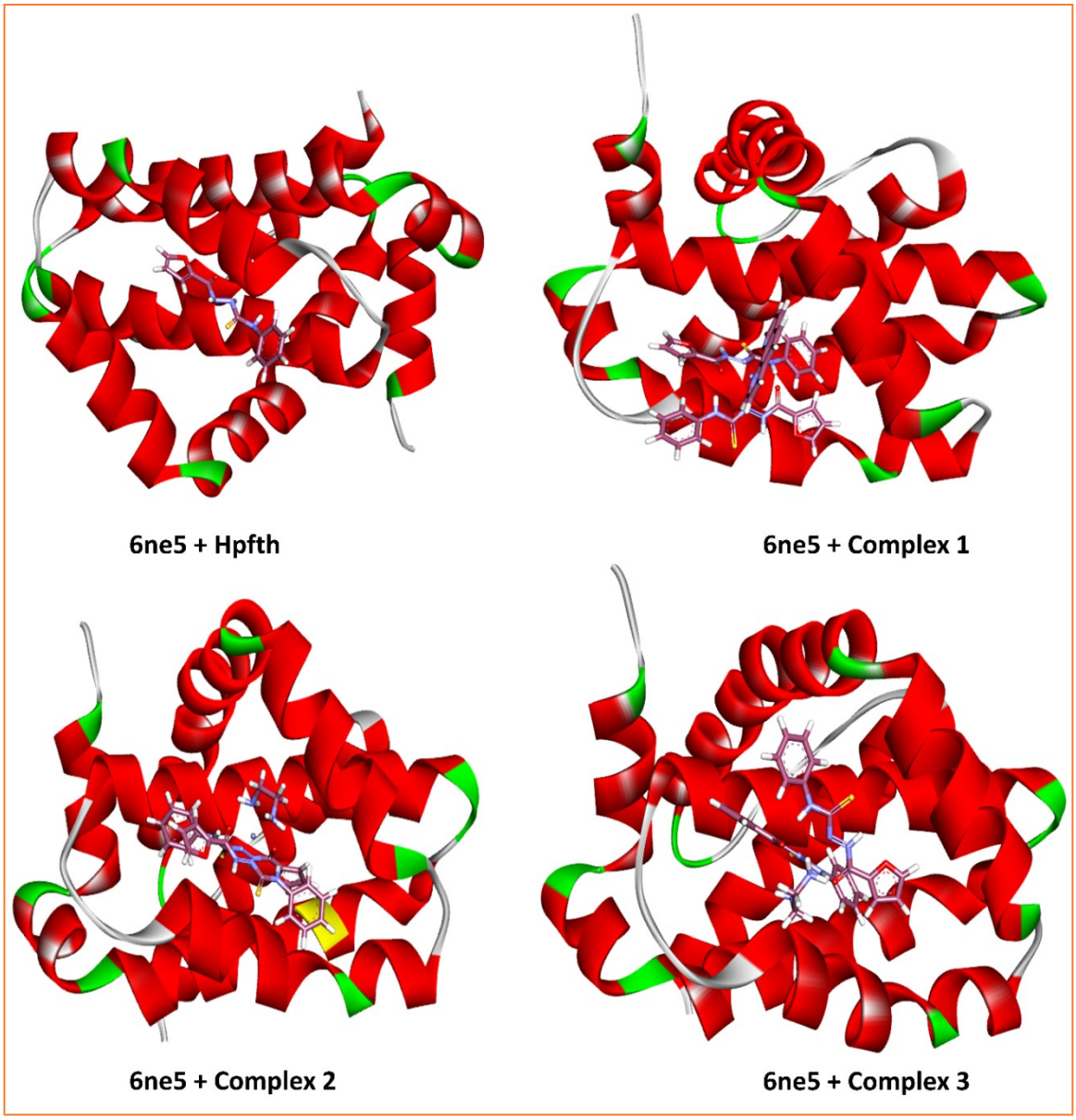

Fig. S8. Docking of Hpfth and complexes with candidate selected target protein 6ne5.

Table ST9: Hydrogen bond level interaction between **Hpfth** and receptor protein within 4 Å*

S. N.	PDB ID	Residues with No.	Residue's atom involved in Hydrogen bonding within 4 Å	**Hpfth** atom involved in Hydrogen bonding within 4Å
1.	6h0w	His90	N	O
		Tyr136	O	O
		Tyr136	O	O
		Tyr181	O	N

*No considerable H-bonding between Hpfth and other receptor proteins is found

Table ST10: Hydrogen bond level interaction between Complex **1** and receptor proteins within 4 Å

S. N.	PDB ID	Residues with No.	Residue's atom involved in Hydrogen bonding within 4 Å	Complex **1** atom involved in Hydrogen bonding within 4Å
1.	6ne5	Val253	N	S
		Val253	N	N
		Arg263	N	O
		Val249	O	H
2.	6h0w	Lys245	N	N
		Lys245	N	O
		Lys245	N	N
3.	6e91	His4	N	S
		Asn11	N	O
		Asn11	N	N
		His4	O	H

Table ST11: Hydrogen bond level interaction between Complex **2** and receptor proteins within 4 Å

S. N.	PDB ID	Residues with No.	Residue's atom involved in Hydrogen bonding within 4 Å	Complex **2** atom involved in Hydrogen bonding within 4Å
1.	6ne5	Met231	S	H
		Met231	S	H
2.	6h0w	Lys245	N	O
		Lys245	N	O
		Glu194	O	H
		Asp139	O	H
3.	6e91	His64	N	S
		Phe231	O	H
		Glu170	O	H

Table ST12: Hydrogen bond level interaction between Complex **3** and receptor proteins within 4 Å*

S. N.	PDB ID	Residues with No.	Residue's atom involved in Hydrogen bonding within 4 Å	Complex **3** atom involved in Hydrogen bonding within 4Å
1.	6ne5	Leu267	N	S
		Val253	O	H
		Val253	O	H
2.	6h0w	Lyc245	N	N
		Lyc245	O	O
		Lyc245	N	N

*No considerable H-bonding between complex 3 and 6e91A receptor proteins is found

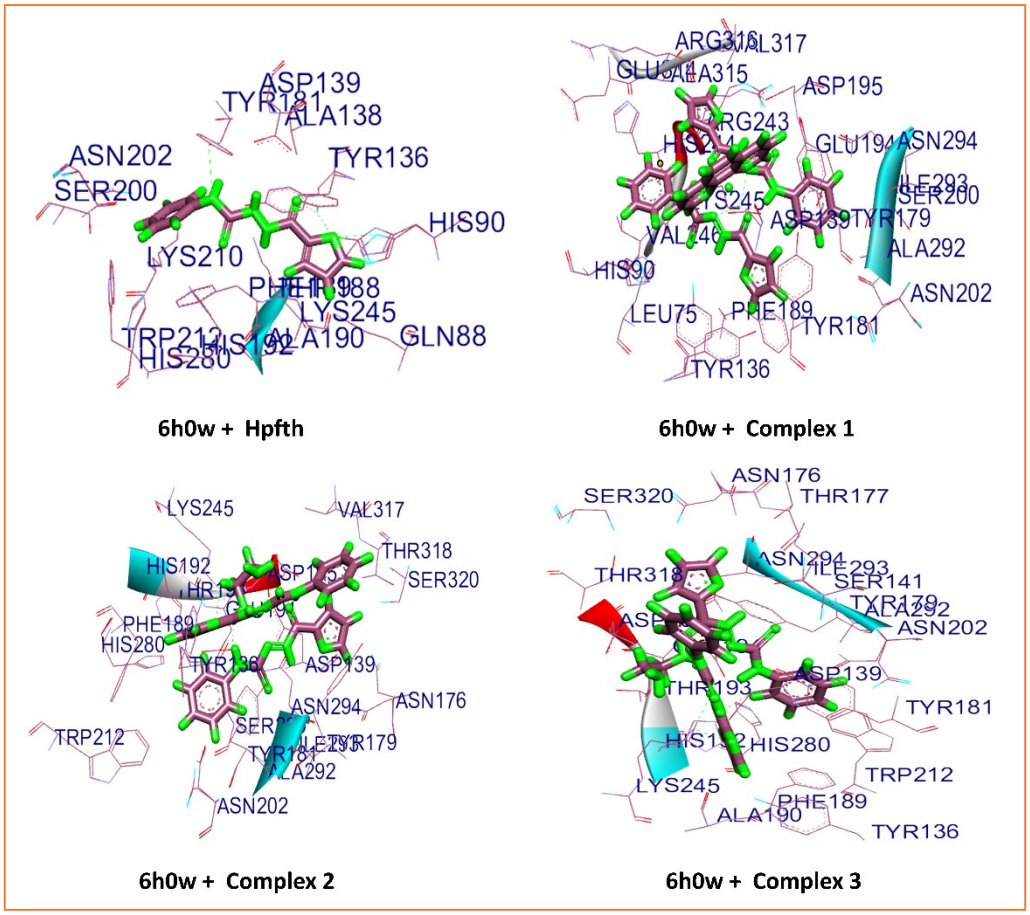

Fig. S9. Hydrogen bond level interaction between Hpfth and complexes with receptor protein 6h0w within 4 Å

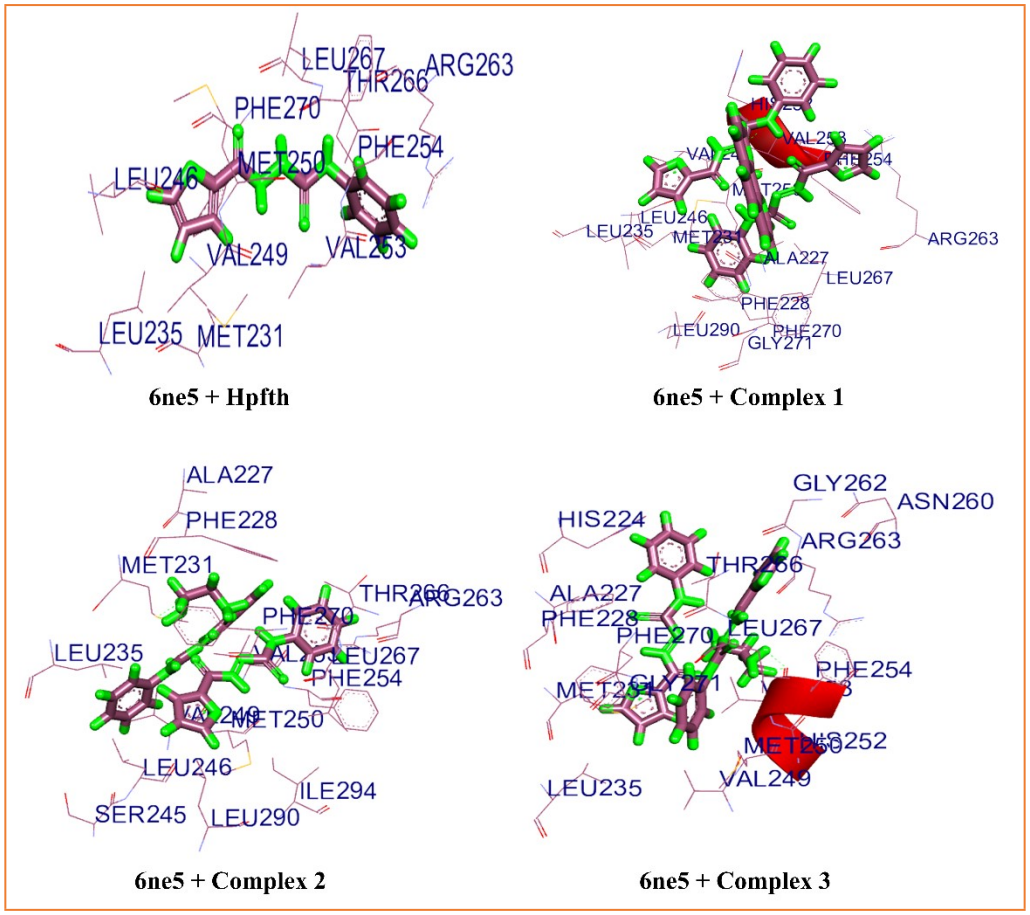

Fig. S10. Hydrogen bond level interaction between Hpfth and complexes with receptor protein 6how within 4 Å

7. Antitumour Studies

7.1 Cell lines and cell culture

K562 (human erythromyeloma cells) and MCF-7 (human breast adenocarcinoma) were purchased from American Type Culture Collection (ATCC), Manassas, USA and was maintained in RPMI 1640 (Invitrogen, Carlsbad, CA) with supplements including 10% fetal bovine serum (Hyclone, Logan, UT), 100 U/ml penicillin and 100 µg/mL streptomycin (Invitrogen, Carlsbad, CA), henceforth considered as a complete medium. Dalton's lymphoma (DL), a murine lymphoma was maintained in complete medium and the peritoneum of BALB/c mice. Human peripheral blood lymphocytes and monocytes were isolated from peripheral blood as described by us before [12].

7.2 Cell Viability study

Short term Effect of free metal, ligand or metal-ligand complex on the viability of tumor cells K562, MCF-7, DL tumor cells and blood lymphocytes and monocytes was evaluated by a colorimetric XTT (sodium 3-[1-(phenylaminocarbonyl)-3,4-tetrazolium]-bis(4-methoxy-6-nitro) assay (Roche, Indianapolis, IN) [12]. Tumor cells were plated (5×10^3 cells/well) in 96-well culture dish and incubated with different concentrations of the above-mentioned compounds or cisplatin and incubated at 37°C, 5% CO_2 for 18 hours. OD was taken at 450 nm in a plate reader (Synergy HT, BioTek, USA). The percent viable cell was calculated employing the formula below:

$$\% \text{ Cell Viability} = \frac{\text{Experimental OD}_{450}}{\text{Control OD}_{450}} \times 100$$

Details of the methodology are given in the supplementary materials and method section.

7.3 Cell growth inhibition assay

Growth inhibitory potential of metal, ligands, and the coordinate complexes against K562, MCF-7, and DL cells was studied by MTT assay. Tumor target cells (5×10^3 cells /well) in a 96 well culture dish was treated with serial concentrations (12.5, 25, 50 µg/ml) of the indicated compounds or cisplatin in a total volume of 200 µL. Following incubation at 37^0C, 5% CO_2 for 48 hours, the proliferation of the tumor cells was assessed by MTT assay using CellTiter 96 kit (Promega, USA). The measurement of absorbance (OD values) was taken at 570 nm in a plate reader (BioTek, USA) [13]. Percent inhibition of the tumor cells was calculated using the under the mentioned formula:

% Growth inhibition = $[1 - \frac{Experimental\ OD_{570}}{Target\ OD_{570}}] \times 100$

The Experimental OD indicates the values of the tumor cells in the presence of the indicated compounds and the Target OD indicates the corresponding values of the tumor cells alone, cultured in medium only.

7.4 Hemolysis assay

Concentration dependent hemolysis of human red blood cells (RBC) in the presence of metal, ligands and the coordinate complexes were performed as described by us before [12].

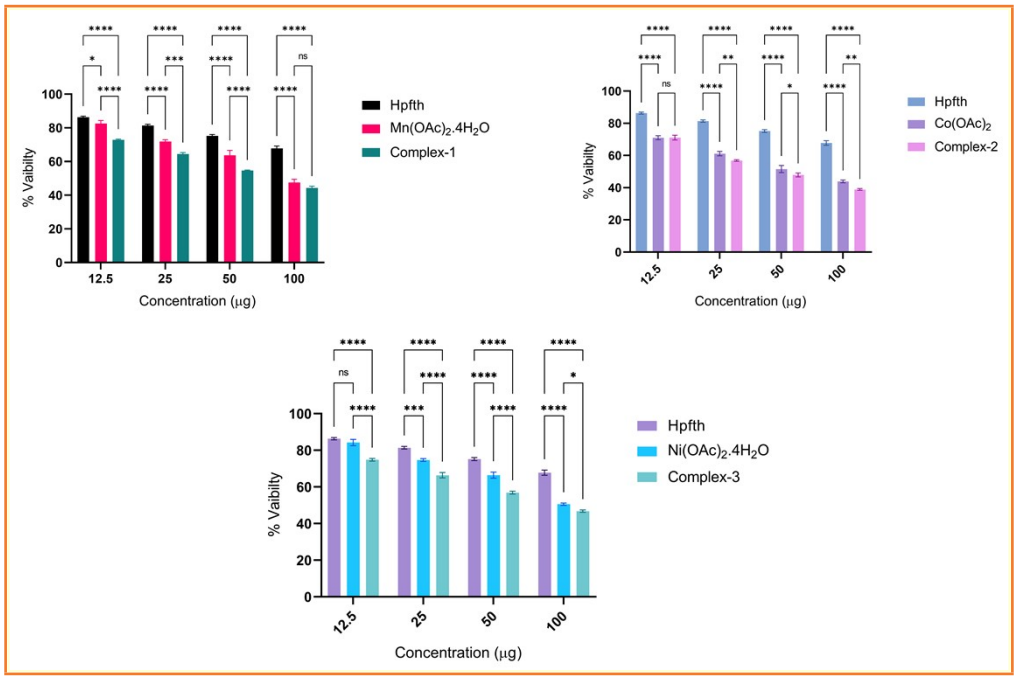

Fig. S11. Viability of peripheral blood lymphocytes in the presence of (A) Mn (B) Co and (C) Ni complexes assessed by 18 hours XTT assay.

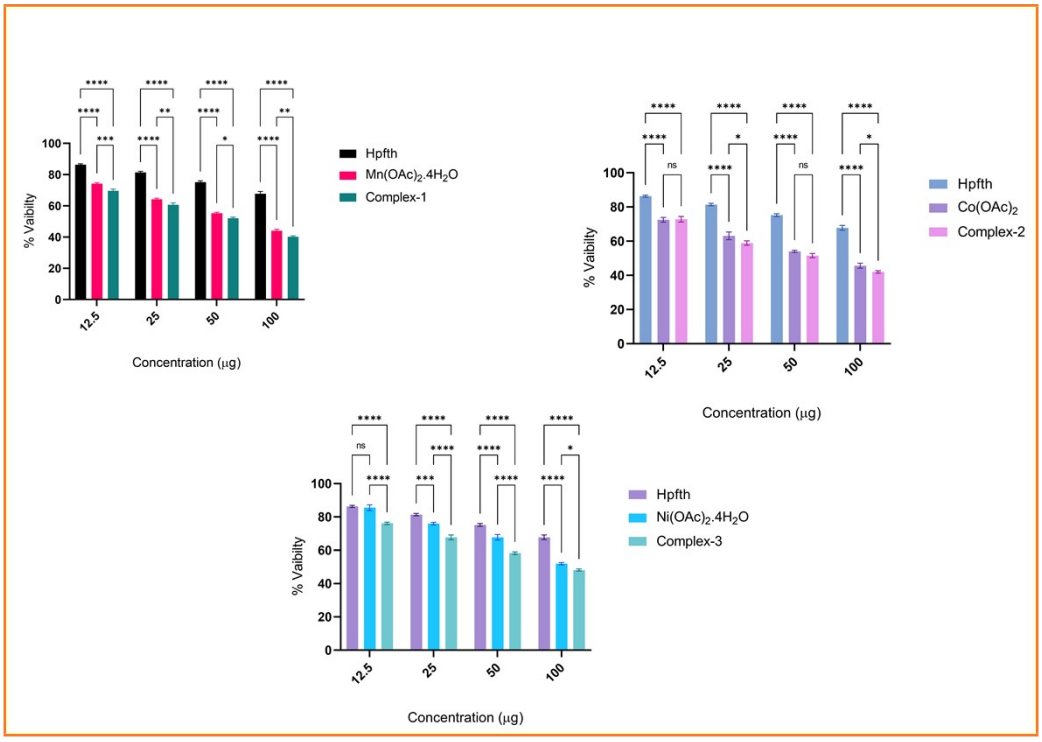

Fig. S12. Viability of peripheral blood monocytes in the presence of (A) Mn, (B) Co and (C) Ni complexes assessed by 18 hours XTT assay.

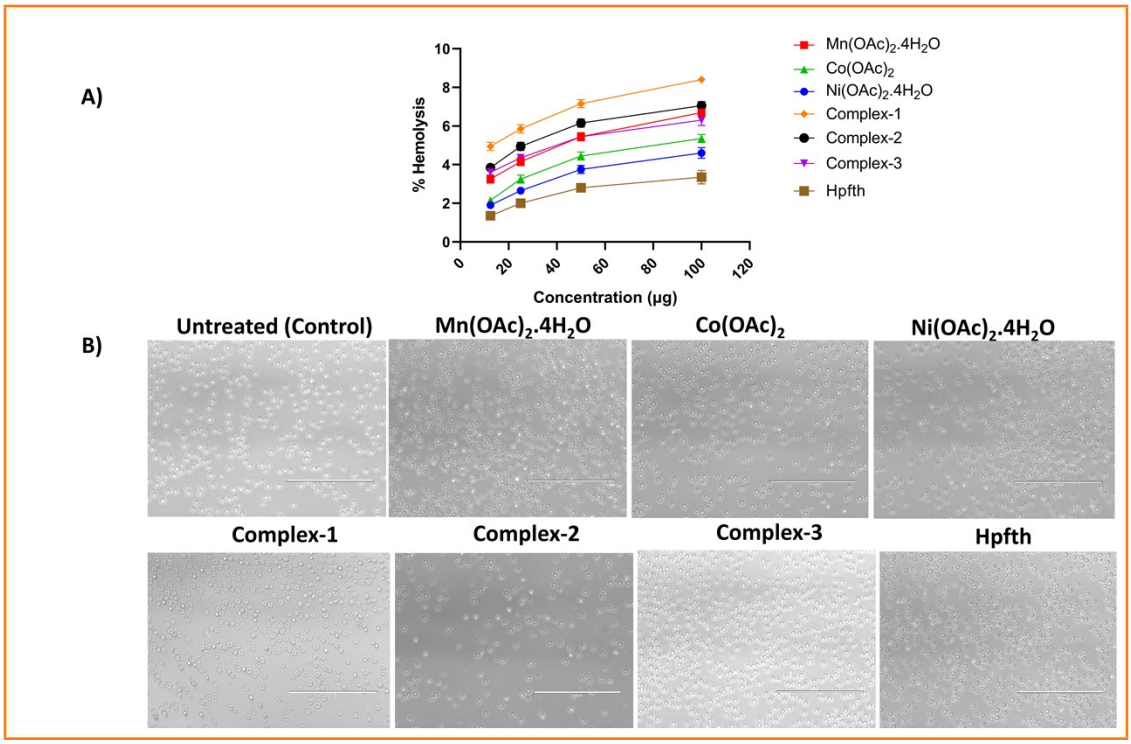

Fig. S13. Concentration dependent hemolysis of RBC in the presence of metals, ligand and metal-ligand complexes (A). Representative bright field photomicrograph of RBC treated with indicated conditions (B).

7.5 Determination of Apoptosis by Acridine orange assay

Microscopic images showed the Apoptosis Analysis Using Acridine Orange Staining. Live cells are bright green with an undisturbed membrane; early apoptotic cells contain green nuclei with chromatin condensation, and late apoptotic cells have orange/red fluorescence [14].

7.6 Clonogenic assay

Clonogenic survival assay was performed according to the method described by us before with some modifications [12]. Cells [10 µL from a stock (1×10^4 cells/ml)] were mixed with 25 µg/ml of the indicated metal, ligands or the coordinate complexes for 24 hours. Cells treated with culture medium were used as control. The cells were thoroughly washed, diluted in a complete medium in the presence of 0.3% noble agar (Difco, Detroit, MI), and plated in a 6-well plate (in triplicate) above a layer of soft agar. Once set, the dishes were flooded with 1.0 ml complete medium and were maintained at 37^0C, 5%CO_2. After 10 days, the total number of colonies/plates was counted. Plating efficiency (PE) and surviving fraction (SF) were calculated as mean ± SD of triplicate determination using the following formula:

$$\text{PE} = \frac{Number\ of\ colonies\ formed}{Number\ of\ cells\ seeded} \times 100$$

The number of colonies that arise after treatment of cells, expressed in terms of PE, is called the surviving fraction (SF).

$$\text{SF} = \frac{Number\ of\ colonies\ formed\ after\ treatment}{Number\ of\ cells\ seeded\ \times\ PE} \times\ 100$$

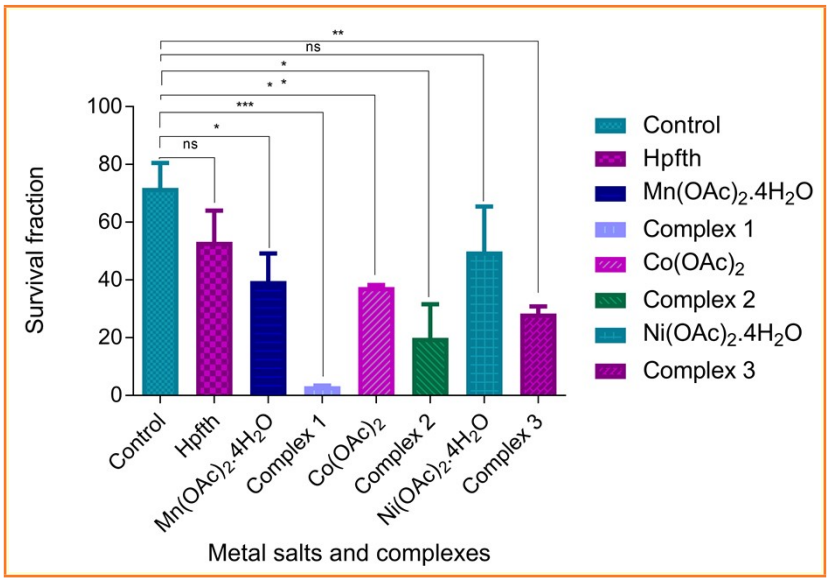

Supporting Fig. S14 Survival fraction of clonogenic DL cells following indicated treatment.

Table S13. IC_{50} analysis of the metal complexes compared with cisplatin in DL, K-562 and MCF-7 cells

Cell line	Hpfth	Cis-Platin	$Mn(OAc)_2.4H_2O$	Complex 1	$Co(OAc)_2$	Complex 2	$Ni(OAc)_2.4H_2O$	Complex 3
DL IC_{50} (µM)	4600 ± 61.43	656 ± 1.03	1900 ± 0.98	296 ± 1.29	3200 ± 1.75	602 ± 3.33	4160 ± 14.2	636.3 ± 2.82
K562 IC_{50} (µM)	2040 ± 17.4	650.9 ± 5.06	930 ± 3.03	26.3 ± 0.43	4700 ± 14.7	507.8 ± 0.85	3410±39.64	118.6 ± 2.46
MCF-7 IC_{50} (µM)	4650±104.46	753.9 ± 3.07	1600 ± 3.19	270 ± 0.07	4700 ± 30.9	604.6 ± 3.49	7900±176.6	605 ± 3.49

8. NMR and HRMS Spectra

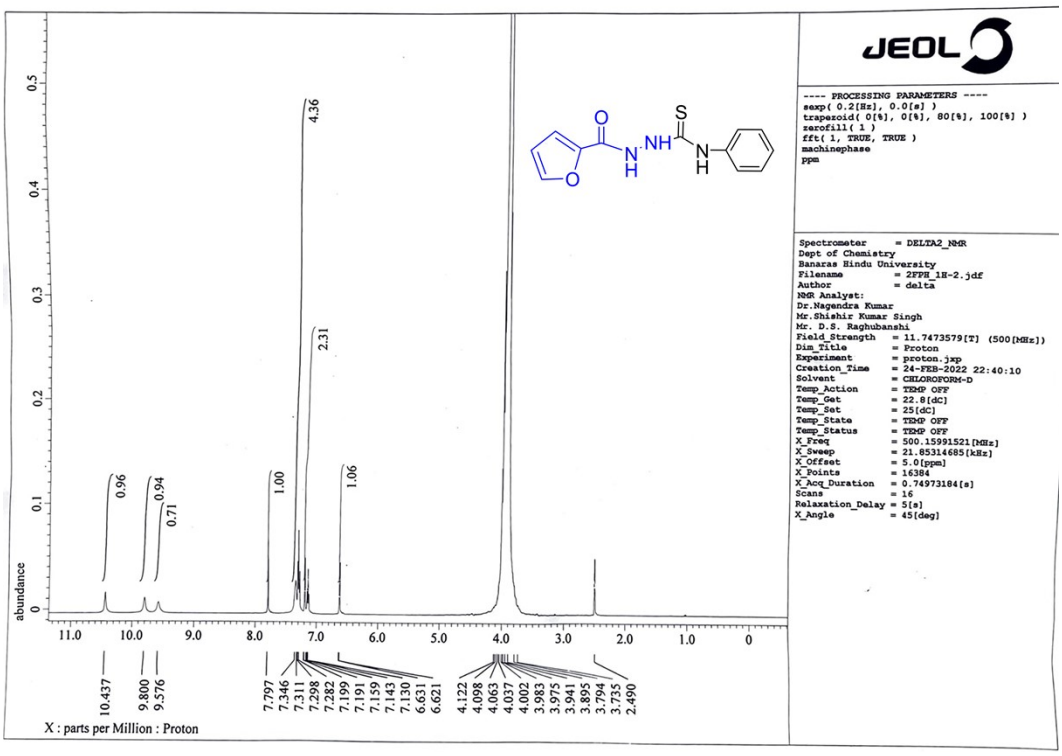

Supporting Fig. 15: ^{1}H NMR spectrum of Hpfth in DMSO-d_6.

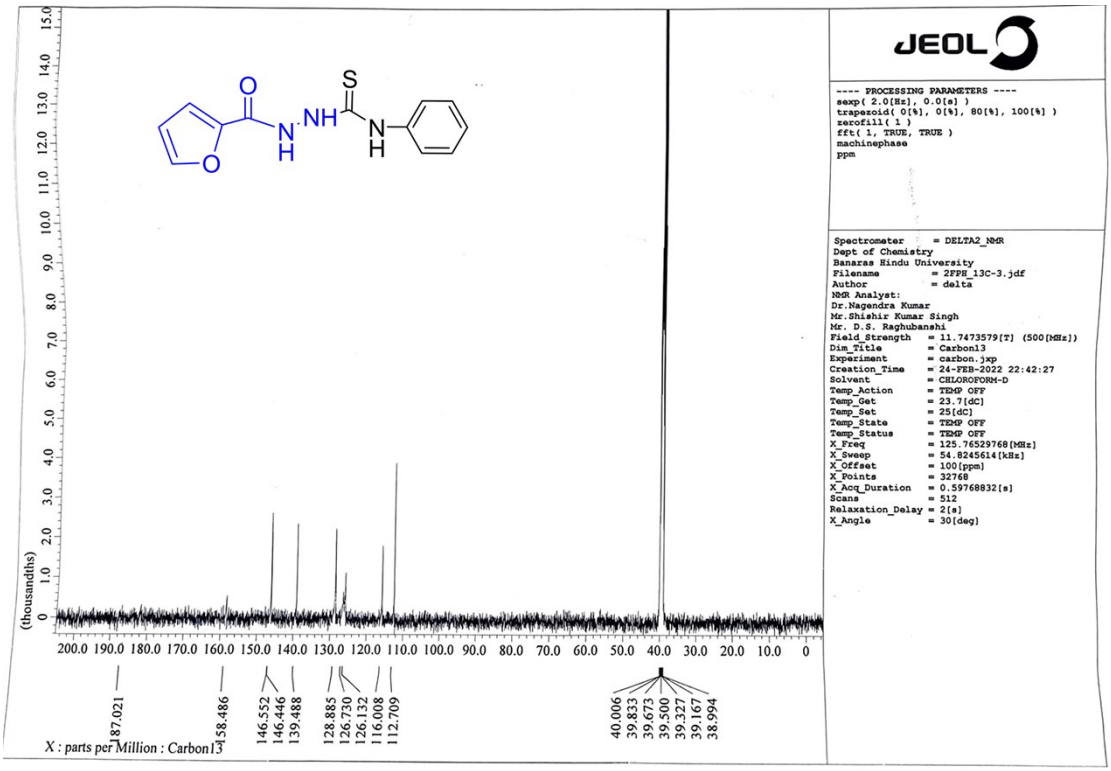

Supporting Fig. 16: ^{13}C NMR spectrum of Hpfth in DMSO-d_6.

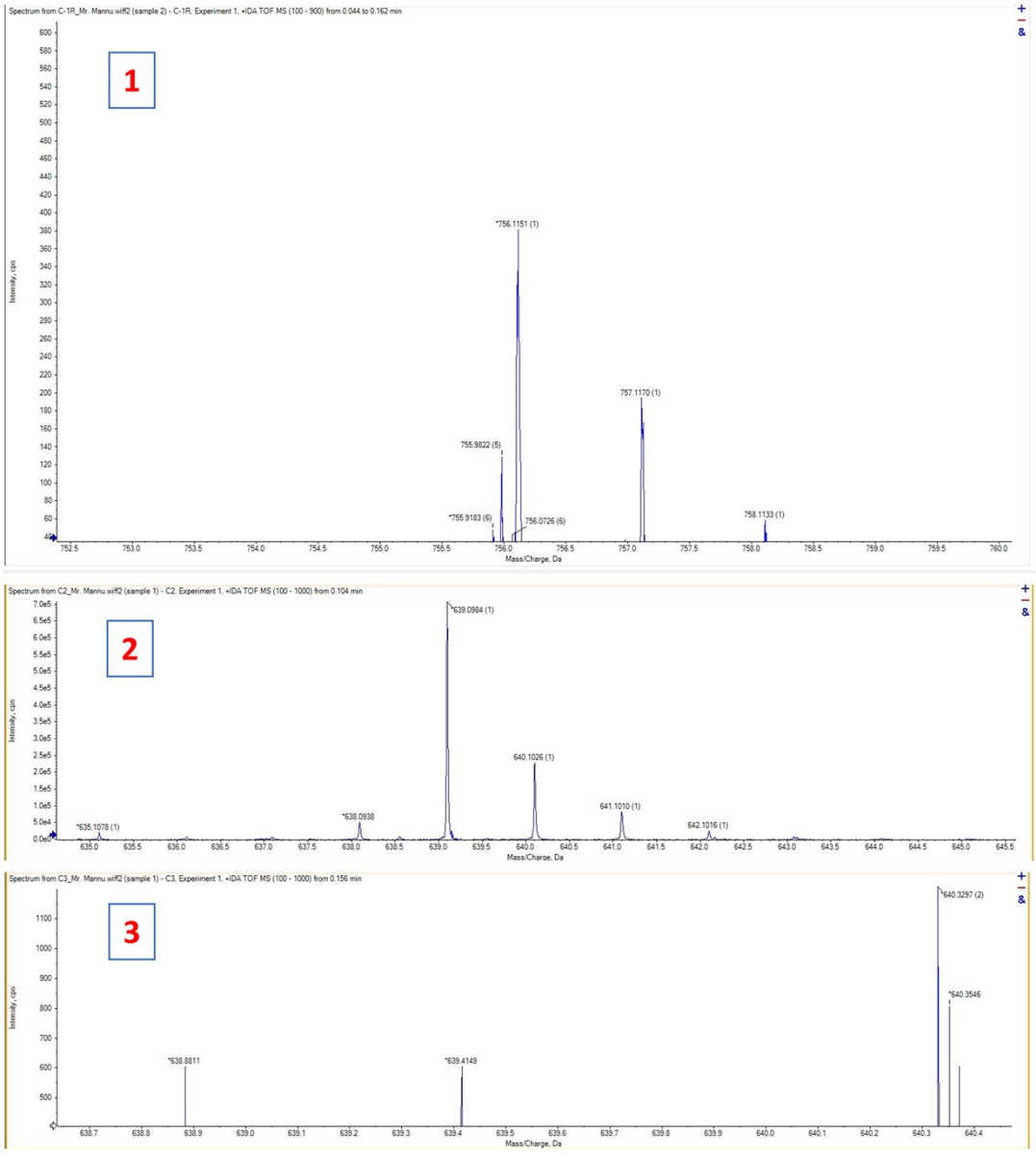

Supporting Fig. 17: ESI-MS Spectra of complexes **1**, **2** and **3**.

8. References

[1] G. M. Sheldrick, *Acta Crystallogr. Section A*, 2008, **64**, 112-122.

[2] C. F. Macrae, I. J. Bruno, J. A. Chisholm, P. R. Edgington, P. McCabe, E. Pidcock, L. Rodriguez-Monge, R. Taylor, J. van de Streek and P.A. Wood, *J. Appl. Cryst.*, 2008, **41**, 466-470.

[3] L. J. Farrugia, *J. Appl. Cryst.*, 2012, **45**, 849-854.

[4] L. J. Bartolottiand and K. Fluchick, in *Reviews in Computational Chemistry*, ed. K. B. Lipkowitz, D. Boyd, VCH, New York, 1996, **7**, 187-216.

[5] A. D. Becke, *J. Chem. Phys.*, 1993, **98**, 5648-6.

[6] C. Lee, W. Yang and R. G. Parr, *Phys. Rev. B: Condens. Matter.*, 1988, **37**, 785-789.

[7] P. J. Hay and W. R. Wadt, *J. Chem. Phys.*, 1985, **82**, 270-283.

[8] M. J. Frisch, G. W. Trucks, H. B. Schlegel, G. E. Scuseria, M. A. Robb, J. R. Cheeseman, G. Scalmani, V. Barone, B. Mennucci, G. Petersson and H. Nakatsuji, *Gaussian 09 Revision d. 01*, Gaussian. Inc., Wallingford CT, 2009.

[9] H. M. Berman, J. Westbrook, Z. Feng, G. Gilliland, T. N. Bhat, H. Weissig, I. N. Shindyalov and P.E. Bourne, *Nucleic Acids Res.*, 2000, **28**, 35-242.

[10] B. Huang, *OMICS A Journal of Integrative Biology*, 2009, **13**, 325-30.

[11] D. S.-Duhovny, Y. Inbar, R. Nussinov and H. J. Wolfson, *Nucleic Acids Res.*, 2005, **33**, W363-W367.

[12] S. K. Hira, A. K. Mishra, B. Ray and P. P. Manna, *PloS one*, 2014, **9**, e94309.

[13] S. K. Hira, K. Ramesh, U. Gupta, K. Mitra, N. Misra, B. Ray and P. P. Manna, *ACS Appl. Mater. Interfaces*, 2015, **7**, 20021-33.

[14] S. Majumdar, S. K. Hira, H. Tripathi, A. SampathKumar, P. P. Manna, S. P. Singh and S. Krishnamurthy, *Ceramics International*, 2021, **47**, 7143-7158.